SUB-10 FS SYNCHRONIZATION IN LASER-PLASMA ACCELERATORS WITH TERAHERTZ FREQUENCY BUNCH MANIPULATION*

A. Amini†[1], L. R. Reid[2], J. K. Jones[2], M. T. Hibberd[1], L. Corner[3], D. M. Graham[1], S. P. Jamison[4], G. Burt[4], R. B. Appleby[1]
Cockcroft Institute, Sci-Tech Daresbury, Keckwick Lane, Warrington, United Kingdom
[1]also at University of Manchester, Oxford Road, Manchester, United Kingdom
[2]also at ASTeC, STFC Daresbury Laboratory, Warrington, United Kingdom
[3]also at University of Liverpool, Brownlow Hill, Liverpool, United Kingdom
[4]also at Lancaster University, Bailrigg, Lancaster, United Kingdom

Abstract

External injection offers a pathway to high-quality electron bunches in laser-plasma accelerators, yet precise synchronization between the drive laser and the injected electron bunch remains a major challenge. We investigate a temporal-locking mechanism using THz-driven waveguides to overcome these synchronization limits. Start-to-end simulations based on the CLARA/FEBE facility show that sub-10 fs synchronization is achievable, corresponding to an eight-fold reduction in arrival time jitter compared to conventional Radio Frequency systems and resulting in an order-of-magnitude improvement in laser-plasma final beam energy stability.

INTRODUCTION

Laser-driven acceleration methods [1–4] offer a promising route toward compact, high-gradient accelerators. In particular, laser-plasma wakefield acceleration (LWFA) has attracted significant attention [5, 6] for producing GeV-class electron beams with gradients of several GV/m. However, the inherently nonlinear laser–plasma interaction limits the generation of stable, high-quality bunches with narrow energy spread and consistent shot-to-shot performance. Such beam quality and stability are essential for applications in high-energy physics (HEP) [7] and free-electron lasers (FEL) [8, 9].

LWFA beams are typically generated via internal (self-) injection, where electrons originate from the background plasma [10–12], offering limited control over the bunch properties. External injection [13–15] provides an alternative by introducing pre-formed electron bunches into the wakefield, enabling improved control of beam quality. Significant efforts [16, 17] have therefore focused on developing reliable external sources, often based on conventional Radio Frequency (RF) injectors.

High-quality electron bunches by LWFA with external injection require femtosecond electron bunches with the precise synchronization of laser and electron beam [18]. Conventional RF injectors typically rely on a magnetic compression system to provide ultrashort electron bunches [19–21] and numerical studies [16] suggest that such systems have critical challenges to produce stable ultrashort electron bunches suitable for LWFA applications, primarily due to nonlinearities and jitter introduced by the RF cavities coming from their mutual independence and asynchronization with the drive laser.

In this paper, we explore a recent temporal-locking concept based on THz-driven waveguides for generating sub-femtosecond electron bunches with precise synchronization for external injection [22], and discuss its advantages over conventional approaches. THz-driven acceleration is a promising approach for next-generation laser-driven accelerators [23], enabled by recent GV/m-level THz sources [24]. THz waveguides have attracted interest for beam manipulation, particularly femtosecond-scale compression [25]. Our recent results [26] show intrinsic temporal locking and reduced timing jitter in high-energy beams, enabling stable high-quality bunch generation and supporting applications such as multi-stage LWFA and storage ring injection.

THz-FREQUENCY CONTROL OF ELECTRON BUNCHES

The concept of THz-controlled electron bunches for external injection into an LWFA takes advantage of the intrinsic synchronization between THz pulse generation and plasma wakefield excitation enabled by using a common laser system to drive both processes, enabling the delivery of stable, high-quality ultrashort bunches. The concept is illustrated schematically in Fig.1(a), where electron bunches (a) from an external RF source (injector and linac) interact with laser-generated THz pulses inside a dielectric-lined waveguide (DLW). The THz-driven DLW (b) acts as a linear energy chirper, imprinting a time-energy correlation on the bunch that intentionally increases its energy spread. This is followed by a magnetic chicane for longitudinal phase-space rotation, compression, and transverse matching into the final stage of laser-plasma acceleration (c).

The THz-driven beam control can be analysed analogously to conventional RF injectors by considering the single-particle dynamics within a theoretical framework. In a rectangular DLW, a set of orthonormal modes known as longitudinal section magnetic (LSM_{mn}) modes are supported, where m and n represent the number of half-wavelength variations along the horizontal and vertical directions. These modes are characterised by the absence of transverse mag-

* Work supported by the Cockcroft Institute and STFC.
† aras.amini@manchester.ac.uk

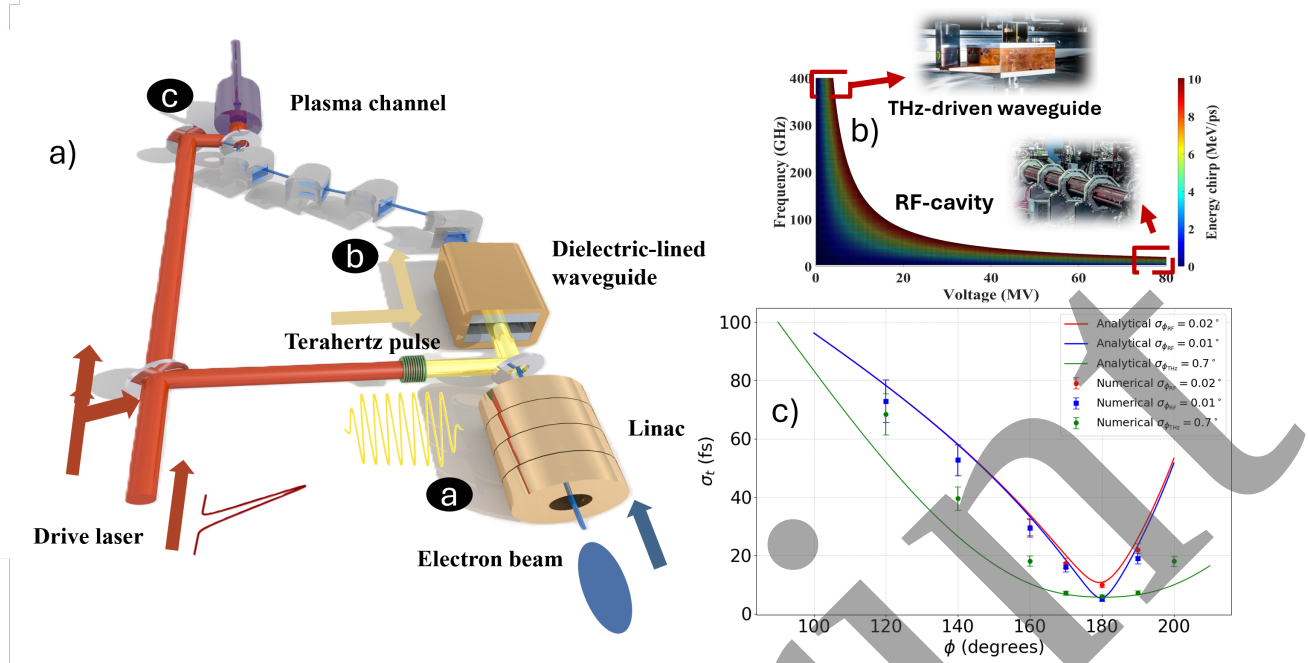

Figure 1: THz-controlled injection for LWFA. (a) Experimental schematic: Electron bunches from an injector are synchronized with laser-driven THz pulses in a dielectric-lined waveguide (DLW). The DLW imprints a linear energy chirp, enabling compression via a magnetic chicane and matching into the plasma stage. (b) Energy chirp scaling: Comparison showing that higher THz frequencies achieve equivalent chirping at significantly lower voltages than conventional RF cavities. (c) Jitter stability: Analytical (lines) and numerical (markers) comparison of arrival time jitter σ_t versus compression phase.

netic (H_y) and electric (E_y) field components at the boundary [27]. Among these, the LSM_{11} mode is most suitable for beam interaction, as it provides a non-zero longitudinal electric field (E_z) on axis. If v_p is the phase velocity of the THz wave and v_e is the velocity of the electron bunch, when phase-velocity matching is achieved ($v_p = v_e$), the electron interacts synchronously with the LSM_{11} mode of the THz field in a dielectric-lined waveguide.

The energy deviation of an electron at longitudinal position ζ_0, relative to a reference particle at ζ_{ref}, after the DLW is given by $\delta = (\gamma_f - \gamma_{\mathrm{ref}})/\gamma_{\mathrm{ref}}$, where γ_{ref} is the Lorentz factor of the reference particle after DLW. Similar to RF cavities, the energy deviation can be expanded as $\delta = \delta_0 + h_1\zeta + h_2\zeta^2 + O(\zeta^3)$, where δ_0 is the initial energy deviation of the single particle relative to the reference particle, mainly defined as uncorrelated energy spread. The coefficients h_1 and h_2 represent the linear and quadratic energy chirps, given by [28]:

$$h_1 = \frac{eVk\sin(\phi_{\mathrm{THz}})}{\gamma_{\mathrm{ref}}}, \quad h_2 = \frac{eVk^2\cos(\phi_{\mathrm{THz}})}{2\gamma_{\mathrm{ref}}}. \tag{1}$$

Here, e is the elementary charge, V is the voltage inside the DLW, and k and ϕ_{THz} are the wavenumber and phase of the THz field, respectively. Although the voltage of THz-driven waveguides is currently limited by a high-power THz source, Fig.1(b) shows how operating at high frequencies compensates for this constraint, allowing for the imprinting of equivalent chirps on electron bunches in a more compact setup compared to RF linacs.

Electrons with varying energies traverse different trajectories in a bend section, so by carefully matching the dispersive parameters of the bend section with the correlated energy spread of the electron bunch, the bunch length can be effectively controlled. A dispersive arc section transforms the longitudinal phase-space coordinates of a particle(ζ_0, δ) to a final position as $\zeta_f = \zeta_0 + R_{56}\delta + T_{566}\delta^2 + O(\delta)$, where R_{56}, and T_{566} are first and second-order longitudinal dispersive parameters of the arc, respectively. Using the energy deviation relation, the final rms bunch length of an electron bunch can be expressed as [28]:

$$\sigma_{\zeta_f} \approx \Big[R_{56}^2\sigma_{\delta_0}^2 + \big[(1 + h_1R_{56})^2 + 2R_{56}\delta_0(h_2R_{56} + h_1^2T_{566})\big]\sigma_{\zeta_i}^2\Big]^{1/2}, \tag{2}$$

where σ_{δ_0} is the rms of the initial uncorrelated energy spread of the bunch. Maximum compression requires matching condition ($R_{56}h_1 = -1$, $T_{566}h_1^2 = h_2R_{56}$), and is favored by smaller R_{56}, and uncorrelated energy spread δ_0, therefore, higher energy chirp h_1.

Conventionally, RF linacs generate the required chirp by operating off-crest ($\phi_{\mathrm{RF}} \in (-\pi, \pi) \setminus \{0\}$), slightly away from the RF peak. Although effective, this approach inherently reduces available energy gain for a given RF power and introduces additional nonlinearities. In contrast, the THz-driven scheme imparts the chirp at the zero-crossing phase ($\phi_{\mathrm{THz}} \simeq \pi/2$), enabling downstream RF linacs to operate

fully on the peak. This configuration provides clear advantages: it maximizes achievable energy gain by RF cavities, significantly reduces the nonlinearities arising from off-crest operation, and ultimately results in a more energy-efficient and compact compression process.

Due to the short plasma wavelength in LWFA, stable acceleration requires precise timing synchronization between the drive laser and the externally injected electron bunch, typically quantified as arrival time jitter. This jitter arises from multiple sources, including photocathode laser timing, RF phase and voltage fluctuations, and magnetic field instabilities. As in bunch compression, it can be mitigated by matching the chicane dispersion to the correlated energy spread of the beam. The arrival time jitter after a magnetic compression stage, dt_f can be expressed analytically as [21]:

$$dt_f \approx \frac{dt_i}{C} + \frac{R_{56}}{c}\left(\frac{e\sin\phi}{E}dV + \frac{eV\cos\phi}{E}d\phi - \frac{dB}{B}\right), \quad (3)$$

where $C = (1 + R_{56}h_1)^{-1}$ represents the compression factor that suppresses the initial jitter dt_i. While high compression ratios theoretically minimize the contribution of the initial timing jitter, the second term of the equation introduces a residual floor determined by fluctuations in the cavity voltage dV, phase $d\phi$, and magnetic field dB. Current state-of-the-art S-band RF systems have demonstrated phase and amplitude stabilities of 0.02° and 0.02%, respectively [29]. Reaching sub-10 fs arrival time jitter requires even more stringent tolerances, typically targeting values below 0.01° and 0.01% [16]. In Fig. 1, the analytical and numerical models compare these advanced RF benchmarks against a proposed THz-driven temporal-locking scheme for a beam energy of 250 MeV and a chicane with $R_{56} = 1.66$ cm. For a baseline initial jitter of 100 fs rms, three linac sections providing a total voltage of 80 MV are utilized to impart the necessary chirp.

The results demonstrate that while the most state-of-the-art RF synchronization ($\sigma_\phi = 0.01°$) can achieve significant suppression near the optimal compression phase, the THz-driven approach offers a superior stability profile. By employing a THz-driven waveguide with a field strength of 100 MV/m over a 17 mm interaction length, the system effectively bypasses the limitations of traditional RF phase fluctuation even when accounting for a sub-10 fs jitter between the laser plasma and the THz pulse [30].

START-TO-END MODELLING

To present the impact of temporal-locking of the bunch, start-to-end (S2E) simulations were performed based on the CLARA/FEBE test facility at the STFC Daresbury Laboratory [31]. The modeling parameters and beamline components are derived from the facility's baseline specifications and reference [22]. Figure 2(a) illustrates the timing jitter suppression achieved by implementing the THz-driven control. The results indicate a reduction in bunch timing jitter to approximately 8 fs rms, representing nearly an eight-fold

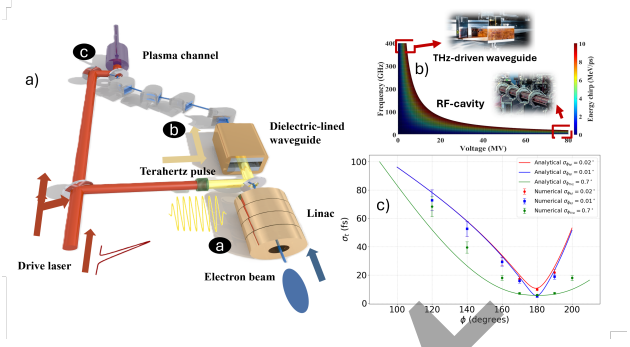

Figure 2: Start-to-end simulation results comparing conventional RF manipulation (blue) and THz-driven control (red) at the CLARA/FEBE facility. (a) Distribution of bunch arrival time jitter $|\sigma_t|$, showing an eight-fold suppression to ~8 fs rms via THz control. (b) Corresponding energy jitter $|\Delta E|$ after laser-plasma interaction, demonstrating an order-of-magnitude improvement in beam energy stability.

improvement in stability compared to the facility's current conventional injector systems (≈ 66.7 fs).

Furthermore, Fig. 2(b) demonstrates the secondary impact of this timing stabilization on the beam's energy profile. The suppression of timing jitter directly mitigates energy fluctuations during the laser-plasma interaction process, leading to a significant enhancement in downstream beam stability. Energy stability improved by an order of magnitude ($\sigma_E \approx 22.6$ MeV vs 332.4 MeV), demonstrating that THz-driven temporal locking is critical for high-precision plasma acceleration.

CONCLUSION

This paper confirms that THz-driven temporal locking provides a robust solution for the sub-femtosecond synchronization required by LWFA. By investigating the mechanism, we demonstrate that shifting the energy chirping process to THz frequencies and employing a common laser-based compression system effectively bypasses the jitter limitations of conventional RF injectors. The resulting order-of-magnitude improvement in beam stability provides the high-precision beam control necessary for future HEP and FEL.

REFERENCES

[1] T. Tajima and J. M. Dawson, "Laser electron accelerator", *Phys. Rev. Lett.*, vol. 43, no. 4, pp. 267–270, 1979. doi:10.1103/PhysRevLett.43.267

[2] A. Picksley *et al.*, "Meter-scale conditioned hydrodynamic optical-field-ionized plasma channels", *Phys. Rev. E*, vol. 102, no. 5, p. 053201, 2020. doi:10.1103/PhysRevE.102.053201

[3] M. T. Hibberd *et al.*, "Acceleration of relativistic beams using laser-generated terahertz pulses", *Nat. Photonics*, vol. 14, no. 12, pp. 755–759, 2020. doi:10.1038/s41566-020-0674-1

[4] M. Litos *et al.*, "High-efficiency acceleration of an electron beam in a plasma wakefield accelerator", *Nature*, vol. 515, no. 7525, pp. 92–95, 2014. doi:10.1038/nature13882

[5] S. P. D. Mangles *et al.*, "Monoenergetic beams of relativistic electrons from intense laser–plasma interactions", *Nature*, vol. 431, no. 7008, pp. 535–538, 2004. doi:10.1038/nature02939

[6] C. G. R. Geddes *et al.*, "High-quality electron beams from a laser wakefield accelerator using plasma-channel guiding", *Nature*, vol. 431, no. 7008, pp. 538–541, 2004. doi:10.1038/nature02900

[7] C. B. Schroeder *et al.*, "Physics considerations for laser-plasma linear colliders", *Phys. Rev. ST Accel. Beams*, vol. 13, no. 10, p. 101301, 2010. doi:10.1103/PhysRevSTAB.13.101301

[8] A. R. Maier *et al.*, "Demonstration scheme for a laser-plasma-driven free-electron laser", *Phys. Rev. X*, vol. 2, no. 3, p. 031019, 2012. doi:10.1103/PhysRevX.2.031019

[9] A. Loulergue *et al.*, "Beam manipulation for compact laser wakefield accelerator based free-electron lasers", *New J. Phys.*, vol. 17, no. 2, p. 023028, 2015. doi:10.1088/1367-2630/17/2/023028

[10] A. Pak *et al.*, "Injection and trapping of tunnel-ionized electrons into laser-produced wakes", *Phys. Rev. Lett.*, vol. 104, no. 2, p. 025003, 2010. doi:10.1103/PhysRevLett.104.025003

[11] E. Esarey *et al.*, "Electron injection into plasma wakefields by colliding laser pulses", *Phys. Rev. Lett.*, vol. 79, no. 14, pp. 2682–2685, 1997. doi:10.1103/PhysRevLett.79.2682

[12] H. Suk *et al.*, "Plasma electron trapping and acceleration in a plasma wake field using a density transition", *Phys. Rev. Lett.*, vol. 86, no. 6, pp. 1011–1014, 2001. doi:10.1103/PhysRevLett.86.1011

[13] C. E. Clayton *et al.*, "Ultrahigh-gradient acceleration of injected electrons by laser-excited relativistic electron plasma waves", *Phys. Rev. Lett.*, vol. 70, no. 1, pp. 37–40, 1993. doi:10.1103/PhysRevLett.70.37

[14] F. Amiranoff *et al.*, "Electron acceleration in Nd-laser plasma beat-wave experiments", *Phys. Rev. Lett.*, vol. 74, no. 26, pp. 5220–5223, 1995. doi:10.1103/PhysRevLett.74.5220

[15] Y. Wu *et al.*, "High-throughput injection–acceleration of electron bunches from a linear accelerator to a laser wakefield accelerator", *Nat. Phys.*, vol. 17, no. 7, pp. 801–806, 2021. doi:10.1038/s41567-021-01188-4

[16] J. Zhu *et al.*, "Sub-fs electron bunch generation with sub-10-fs bunch arrival-time jitter via bunch slicing in a magnetic chicane", *Phys. Rev. Accel. Beams*, vol. 19, no. 5, p. 054401, 2016. doi:10.1103/PhysRevAccelBeams.19.054401

[17] A. R. Rossi *et al.*, "External-injection experiment at SPARC_LAB", *Phys. Procedia*, vol. 52, pp. 90–99, 2014. doi:10.1016/j.phpro.2014.06.016

[18] A. J. W. Reitsma *et al.*, "Efficiency and energy spread in laser-wakefield acceleration", *Phys. Rev. Lett.*, vol. 94, no. 8, p. 085004, 2005. doi:10.1103/PhysRevLett.94.085004

[19] P. Piot *et al.*, "Longitudinal phase space manipulation in energy recovering linac-driven free-electron lasers", *Phys. Rev. ST Accel. Beams*, vol. 6, no. 3, p. 030702, 2003. doi:10.1103/PhysRevSTAB.6.030702

[20] Y. Sun *et al.*, "X-band RF-driven free-electron laser driver with optics linearization", *Phys. Rev. ST Accel. Beams*, vol. 17, no. 11, p. 110703, 2014. doi:10.1103/PhysRevSTAB.17.110703

[21] P. Craievich *et al.*, "Modeling and experimental study to identify arrival-time jitter sources in the presence of a magnetic chicane", *Phys. Rev. ST Accel. Beams*, vol. 16, no. 9, p. 090401, 2013. doi:10.1103/PhysRevSTAB.16.090401

[22] A. Amini *et al.*, "Controlling external injection in laser-plasma accelerators with terahertz frequency bunch manipulation", arXiv preprint arXiv:2604.16059, 2026. doi:10.48550/arXiv.2604.16059

[23] E. A. Peralta *et al.*, "Demonstration of electron acceleration in a laser-driven dielectric microstructure", *Nature*, vol. 503, no. 7474, pp. 91–94, 2013. doi:10.1038/nature12664

[24] J. A. Fülöp *et al.*, "Laser-driven strong-field terahertz sources", *Adv. Opt. Mater.*, vol. 8, no. 3, p. 1900681, 2020. doi:10.1002/adom.201900681

[25] L. Zhao *et al.*, "Femtosecond relativistic electron beam with reduced timing jitter from THz-driven beam compression", *Phys. Rev. Lett.*, vol. 124, no. 5, p. 054802, 2020. doi:10.1103/PhysRevLett.124.054802

[26] M. T. Hibberd *et al.*, "Terahertz control of relativistic electron beams for femtosecond bunching and laser-synchronized temporal locking", arXiv preprint arXiv:2508.20685, 2025. doi:10.48550/arXiv.2508.20685

[27] L. Xiao, W. Gai, and X. Sun, "Field analysis of a dielectric-loaded rectangular waveguide accelerating structure", *Phys. Rev. E*, vol. 65, no. 1, p. 016505, 2001. doi:10.1103/PhysRevE.65.016505

[28] W. K. Lau, M. C. Chou, N. Y. Huang, A. P. Lee, and J. Wu, "Design of a Dogleg Bunch Compressor with Tunable First-Order Longitudinal Dispersion", in *Proc. FEL'17*, Santa Fe, NM, USA, Aug. 2017, pp. 309–312. doi:10.18429/JACoW-FEL2017-TUP031

[29] Z. G. Geng *et al.*, "RF Jitter and Electron Beam Stability in the SwissFEL Linac", in *Proc. FEL'19*, Hamburg, Germany, Aug. 2019, pp. 400–403. doi:10.18429/JACoW-FEL2019-WEP037

[30] P. Cinquegrana *et al.*, "Optical beam transport to a remote location for low jitter pump-probe experiments with a free-electron laser", *Phys. Rev. Accel. Beams*, vol. 17, no. 4, p. 040702, 2014. doi:10.1103/PhysRevSTAB.17.040702

[31] S. Angal-Kalinin *et al.*, "Design, specifications, and first beam measurements of the compact linear accelerator for research and applications front end", *Phys. Rev. Accel. Beams*, vol. 23, no. 4, p. 044801, 2020. doi:10.1103/PhysRevAccelBeams.23.044801